

Activation Entropy as a Key Factor Controlling the Memory Effect in Glasses

Lijian Song,^{1,2} Wei Xu,^{1,2} Juntao Huo^{1,2}, Fushan Li,³ Li-Min Wang,⁴ M. D. Ediger⁵, and Jun-Qiang Wang^{1,2,3,*}

¹CAS Key Laboratory of Magnetic Materials and Devices, and Zhejiang Province Key Laboratory of Magnetic Materials and Application Technology, Ningbo Institute of Materials Technology and Engineering, Chinese Academy of Sciences, Ningbo 315201, China

²Center of Materials Science and Optoelectronics Engineering, University of Chinese Academy of Sciences, Beijing 100049, China

³School of Materials Science and Engineering, Zhengzhou University, Zhengzhou 450001, China

⁴State Key Lab of Metastable Materials Science and Technology, and College of Materials Science and Engineering, Yanshan University, Qinhuangdao, Hebei 066004, China

⁵Department of Chemistry, University of Wisconsin-Madison, Madison, Wisconsin 53706, USA



(Received 14 April 2020; accepted 2 September 2020; published 21 September 2020)

As opposed to the common monotonic relaxation process of glasses, the Kovacs memory effect describes an isothermal annealing experiment, in which the enthalpy and volume of a preannealed glass first increases before finally decreasing toward equilibrium. This interesting behavior has been observed for many materials and is generally explained in terms of heterogeneous dynamics. In this Letter, the memory effect in a model Au-based metallic glass is studied using a high-precision high-rate calorimeter. The activation entropy (S^*) during isothermal annealing is determined according to the absolute reaction rate theory. We observe that the memory effect appears only when the second-annealing process has a large S^* . These results indicate that a large value of S^* is a key requirement for observation of the memory effect and this may provide a useful perspective for understanding the memory effect in both thermal and athermal systems.

DOI: 10.1103/PhysRevLett.125.135501

Glasses are nonequilibrium systems with various types of relaxation processes [1–5], all of which contribute toward equilibration of the glass. Glasses retain memory of their thermal history and this can lead to surprisingly complex equilibration paths. When a glass is annealed sequentially at two temperatures, i.e., first at low temperature and then at a higher temperature, the glass can “rejuvenate” during the second step annealing, which was observed by Kovacs in the 1960s [6]. In this process, known as the *memory effect*, the enthalpy and volume first increase during the second annealing (moving in the direction of a younger glass) before finally decreasing as equilibrium is approached [7–30]. It is intriguing that such a two-step annealing protocol can achieve superior magnetic properties in metallic glasses [31] in comparison to a single-step annealing process.

Phenomenological models such as the Tool-Narayananaswamy-Moynihan (TNM) model have been used to describe the Kovacs memory effect in glasses [7–13]. The TNM model suggests that the memory effect derives from the heterogeneous nature of glass which has been related to the nonexponential nature of the alpha relaxation process [32,33]. In the TNM model, the memory effect cannot be obtained for homogeneous dynamics (exponential relaxation) and experimental data support the view that dynamic heterogeneity is correlated with the strength of the memory effect [11,14,15,34]. The TNM model involves

activation enthalpies and can qualitatively fit thermally activated memory effects in polymer glasses [11,14] and oxide glasses [9,21], it provides no insight into the memory effects in athermal disordered systems [22–26,34], e.g., crumpled papers [22,23], frictional interface [24], and granular materials [25,26]. As the memory effect seems to be quite general in complex disordered systems, it is worthwhile to look for underlying physical mechanisms that encompass both thermal and athermal systems.

In this Letter, the memory effect of a model metallic glass (MG) ($\text{Au}_{49}\text{Cu}_{26.9}\text{Ag}_{5.5}\text{Pd}_{2.3}\text{Si}_{16.3}$) with good glass forming ability, and low glass transition temperature and liquidus temperature [4,35–39] is studied using a high-precision high-rate differential scanning calorimeter. The influence of the annealing temperature and the annealing time has been studied systematically. Absolute reaction rate theory is applied to calculate the activation entropy S^* and the activation enthalpy H^* during relaxation process. It is found that the S^* plays a key role in triggering the Kovacs memory effect in this metallic glass and it may also provide a general way of describing memory effects that encompasses athermal systems.

The enthalpy relaxation of the Au-based MG was measured using a Flash DSC (Flash DSC 1, Mettler Toledo [40]). A high cooling rate of $R_c = 10\,000$ K/s was applied to obtain a fully glassy sample (critical cooling rate for glass formation ~ 1000 K/s [38]). The glass

transition temperature (T_g) upon cooling is about 430 K. To characterize the enthalpy relaxation process, the sample was annealed isothermally and then the heat flow for the annealed sample was measured upon heating (see Fig. S1 [41]). The heat flow difference between the annealed sample and the as-cooled sample is integrated to obtain the relaxation enthalpy. To examine the Kovacs memory effect, the sample was held at the first annealing temperature ($T_1 = 348, 363, \text{ or } 373 \text{ K}$), and then the temperature was quickly increased to the second-annealing temperature $T_2 = 383 \text{ K}$.

Figure 1 shows the behavior of the enthalpy for single-step and two-step annealing protocols for the Au-based MG. For single temperature annealing at 383 K, the enthalpy decreases monotonically toward equilibrium enthalpy with increasing time, as shown in Fig. 1(a). For a two-step annealing process starting with $t_1 = 50 \text{ s}$ at $T_1 = 383 \text{ K}$, and followed by annealing at $T_2 = 373 \text{ K}$, the enthalpy also decreases monotonically with increasing t_2 , as shown in Fig. 1(b). However, for a two-step annealing process starting with $t_1 = 50 \text{ s}$ at $T_1 = 373 \text{ K}$, and then subsequent annealing at $T_2 = 383 \text{ K}$, the enthalpy does not decrease monotonically but first increases to a higher energy state and then decreases toward the equilibrium state, as shown in Fig. 1(c). To better illustrate the relaxation peak, two-dimensional contour images of heat flow are shown in Figs. 1(d)–1(f). When the glass is isothermally annealed at 383 K, the heat flow increases monotonically and the peak shifts to a higher temperature along with the increase of annealing time, as shown in Fig. 1(d). When the glass was preannealed at $T_1 = 383 \text{ K}$ for $t_1 = 50 \text{ s}$ before the isothermal annealing at $T_2 = 373 \text{ K}$, the heat flow also increases monotonically and the peak shifts to higher temperature along with the increase of annealing time t_2 , as shown in Fig. 1(e) (images for preannealing time $t_1 = 0.1\text{--}100 \text{ s}$ are shown in Fig. S2 [41]). However, if the glass is preannealed at a lower temperature, e.g., $T_1 = 373 \text{ K}$ for $t_1 = 50 \text{ s}$ before the second-step annealing at $T_2 = 383 \text{ K}$, the heat flow first decreases and then increases along with t_2 , as shown in Fig. 1(f) (images for preannealing time $t_1 = 0.1\text{--}100 \text{ s}$ are shown in Fig. S3 [41]).

To describe the relaxation characteristics of two-step annealing processes of the sample, the phenomenological

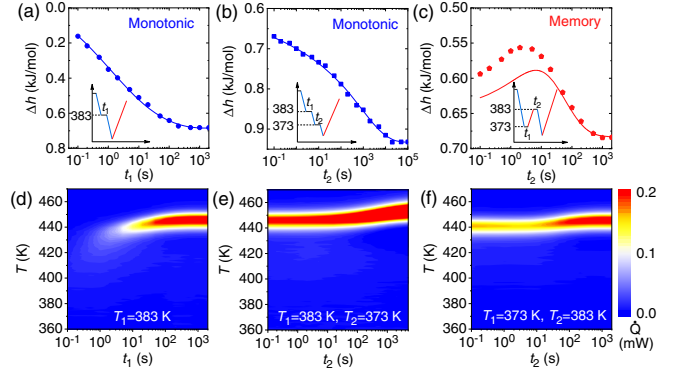


FIG. 1. Enthalpy changes for a Au-based MG during annealing. (a) The enthalpy change Δh at $T_1 = 383 \text{ K}$ versus annealing time t_1 . Inset is the thermal protocol of single-step annealing treatment. Solid curve is for guiding eyes. (b) The enthalpy change of sample preannealed at $T_1 = 383 \text{ K}$ for $t_1 = 50 \text{ s}$ and then annealed at $T_2 = 373 \text{ K}$ for $t_2 = 0.1\text{--}100\,000 \text{ s}$. Inset is the thermal protocol. Solid curve is for guiding eyes. (c) The enthalpy change of sample preannealed at $T_1 = 373 \text{ K}$ for $t_1 = 50 \text{ s}$ and then being annealed at $T_2 = 383 \text{ K}$ for $t_2 = 0.1\text{--}2000 \text{ s}$. Inset is the thermal protocol. Solid curve is the TNM model fitting result. (d) Two-dimensional contours of the relaxation heat flows (\dot{Q}) at $T_1 = 383 \text{ K}$. (e) Two-dimensional contours of the relaxation heat flows at $T_2 = 373 \text{ K}$ for the sample preannealed at $T_1 = 383 \text{ K}$ for $t_1 = 50 \text{ s}$. (f) Two-dimensional contours of the relaxation heat flows at $T_2 = 383 \text{ K}$ for the sample preannealed at $T_1 = 373 \text{ K}$ for $t_1 = 50 \text{ s}$.

TNM model was used to fit the evolution of enthalpy recovery with time (see details in Supplemental Materials [41]). For single-step annealing condition, it was given by [9]:

$$\frac{h_{\text{tot}} - h(t)}{h_{\text{tot}}} = \frac{T_f - T_a}{T_0 - T_a} = 1 - \exp\left[-\left(\int_0^t \frac{dt}{\tau}\right)^\beta\right]. \quad (1)$$

Here, T_f is the fictive temperature and $T_0 = 430 \text{ K}$ represents the starting point of the equilibrium supercooled liquid. The parameters τ and β characterize the timescale and the nonexponential nature of the response function ($0 < \beta \leq 1$). For two-step annealing conditions, the enthalpy change is given by [9]

$$\frac{h_{\text{tot}} - h(t)}{h_{\text{tot}}} = \frac{T_f - T_2}{T_0 - T_2} = 1 + \frac{(T_1 - T_0)}{T_0 - T_2} \times \left\{ 1 - \exp\left[-\left(\sum_{i=1}^{n_1} \frac{\Delta t}{\tau_i} + \sum_{j=n_1}^n \frac{\Delta t}{\tau_j}\right)^\beta\right]\right\} + \frac{(T_2 - T_1)}{T_0 - T_2} \left\{ 1 - \exp\left[-\left(\sum_{j=n_1}^n \frac{\Delta t}{\tau_j}\right)^\beta\right]\right\}. \quad (2)$$

Here, the decay of nonexponential response function is represented as a series of small time increments. The structure relaxation time τ_i has the form

$$\tau_i = \exp\left\{\ln(A) + (xH^*)/(RT_a)\right. \\ \left. + [(1-x)H^*]/(RT_{(f,i-1)})\right\}, \quad (3)$$

where A is constant, x is the nonlinear parameter ($0 < x \leq 1$), and H^* is the activation enthalpy of the relaxation process. The two-step annealing data were fitted with $H^* = 164$ kJ/mol, $A = 6 \times 10^{-22}$ s, $x = 0.6$, and $\beta = 0.43$, with fits shown in Figs. 1 and 2. The TNM model can qualitatively capture the two-step annealing conditions with these fixed parameters, as shown in Fig. 1(c).

To examine the influence of the preannealing temperature in the two-step annealing protocol on the memory effect, Figs. 2(a)–2(c) compare enthalpy relaxation at $T_2 = 383$ K after preannealing at three different temperatures ($T_1 = 348, 363,$ and 373 K). At all T_1 , the enthalpy change Δh decays monotonically with t_2 for short preannealing. When the preannealing time t_1 is large enough, the enthalpy exhibits the memory effect during subsequent annealing. For the same preannealing time (e.g., 100 s), the enthalpy rejuvenates to maximum value at a shorter time when it is preannealed at lower temperatures. Figure 2(d)

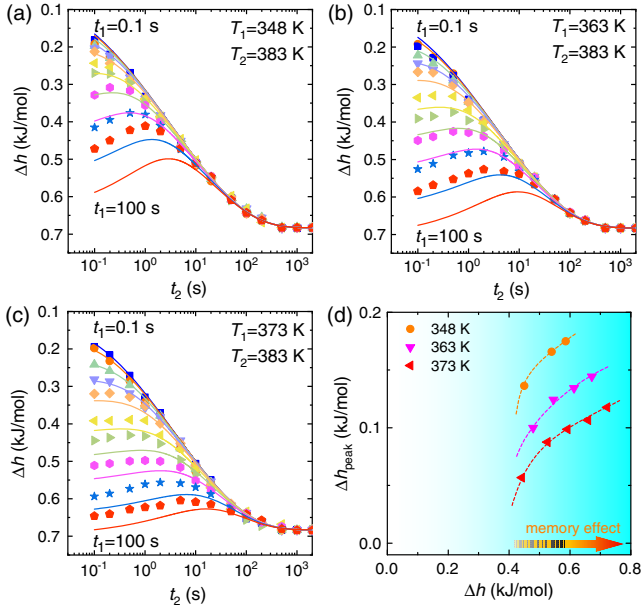


FIG. 2. Enthalpy changes for two-step annealing experiments, with fit results from TNM model (solid lines). (a) The enthalpy change following annealing at $T_2 = 383$ K for the sample preannealed at $T_1 = 348$ K for $t_1 = 0.1, 0.2, 0.5, 1, 2, 5, 10, 20, 50, 100$ s. (b) The enthalpy change following annealing at $T_2 = 383$ K for the sample preannealed at $T_1 = 363$ K for $t_1 = 0.1, 0.2, 0.5, 1, 2, 5, 10, 20, 50, 100$ s. (c) The enthalpy change when being annealed at $T_2 = 383$ K for the sample preannealed at $T_1 = 373$ K for $t_1 = 0.1, 0.2, 0.5, 1, 2, 5, 10, 20, 50, 100$ s. (d) The strength of memory effect (Δh_{peak}) versus enthalpy evolution (Δh) during the first annealing step at $T = 348, 363, 373$ K. Δh_{peak} is obtained by subtracting the initial enthalpy from the peak enthalpy. The memory effect appears only for Δh greater than about 0.4 kJ/mol. The solid symbols represent experimental data in which the memory effect was observed. The dashed lines are for guides for the eyes.

shows the relationship between Δh and the strength of memory effect (Δh_{peak} , obtained by subtracting the peak enthalpy by the initial enthalpy). It is valuable to note that the TNM model fitting result shows qualitatively the wrong curvature in comparison to the experimental results (see details in Supplemental Material [41]). The memory strength in the TNM model changes slowly at small Δh but fast at large Δh . However, the experimental results indicate that the memory effect vanishes quickly when Δh is smaller than 0.4 kJ/mol [corresponding to the pink hexagons, green triangles, and yellow triangles data in Figs. 2(a)–2(c), respectively].

According to the absolute reaction rate theory [42] (see details in Supplemental Material [41]), a relaxation process can be described by

$$\ln \frac{R_h}{T_p^3} = -\frac{H^*}{RT_p} + \ln \frac{kR}{h_p} + \ln \frac{1}{H^*} + \frac{S^*}{R}, \quad (4)$$

where k is the Boltzmann constant, R is the gas constant, h_p is Planck constant, H^* is the activation enthalpy, and S^* is the activation entropy. As shown in Fig. 3(a), Eq. (4) fits the relaxation peak temperature very well for single-step annealing. Figure 3(b) shows the evolution of H^* and S^* as a function of the annealing time. At short annealing times, H^* is about 90 kJ/mol, while H^* increases to about 150 kJ/mol at longer aging time. As a consistency check, we verified that the activation energy (ΔE) in a Kissinger plot, i.e., R_h/T^2 versus $1/T$ [43], is equal to $H^* + RT_p$ [47] (see Fig. S4 [41]). Figure 3(b) shows that S^* evolves dramatically with increasing annealing time. At short annealing times, S^* is close to zero (about 15 J/mol K) indicating that the activated process is primarily enthalpic. However, as the annealing time increases, S^* increases up to roughly 150 J/mol K, indicating a strong entropic component to the structural relaxation process; in this regime, a large number of paths allow escape from the initial state [48].

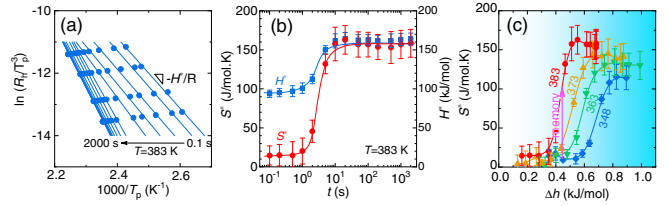


FIG. 3. Absolute rate theory analysis of annealing kinetics. (a) The peak temperature and heating rate are used to extract the activation enthalpy H^* for various annealing times during annealing at 383 K. (b) The evolution of H^* and the activation entropy S^* with annealing time at 383 K. (c) S^* as a function of enthalpy change for single-step annealing at $T = 348, 363, 373, 383$ K. The arrow shows that the memory effect appears only if the glass jumps from low temperature (with a small S^*) to high temperature (with a big S^*).

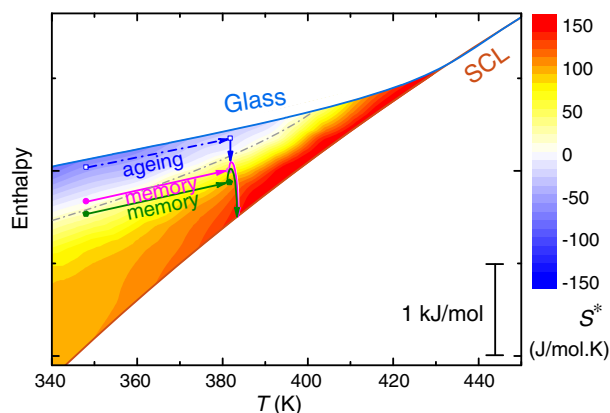


FIG. 4. Schematic map of enthalpy changes during glass annealing. As the enthalpy decreases during isothermal annealing at low temperature, the as-cooled glass first experiences a small S^* stage and then transitions into a large S^* stage. When the preannealed glass jumps to higher temperature, the enthalpy continues to decrease if the jump reaches a relaxation stage with small S^* , but there is a memory effect if the jump reaches a relaxation stage with large S^* . The color map represents the value of S^* . Open blue squares: the sample preannealed at $T = 348$ K for 1 s does not exhibit the memory effect at 383 K. Filled pink circles: the sample preannealed at $T = 348$ K for 20 s exhibits memory effect at 383 K. Filled green pentagons: the sample preannealed at $T = 348$ K for 100 s exhibits memory effect at 383 K.

These experiments reveal a striking correlation between the value of the activation entropy and the memory effect. We illustrate this by considering the evolution of S^* versus the enthalpy change during isothermal annealing at representative temperatures $T = 348, 363, 373,$ and 383 K, as shown in Fig. 3(c). A representative temperature jump that gives rise to the memory effect is shown by the pink arrow, which corresponds to the data of the same color in Fig. 2(a) (and the pink arrow in Fig. 4). The pink arrow is vertical on this graph as Δh does not change during a rapid temperature jump. In this example and in all other cases explored in this work, the memory effect occurs only when the temperature jump moves the glass into a state with a larger value of S^* . No memory effect is observed if the jump occurs into a smaller S^* state. This can be seen by comparing the transition seen in the experimental data in Fig. 2(d) to the transition observed in the red curve of Fig. 3(c); the memory effect is only observed when Δh in the first annealing step exceeds 0.4 kJ/mol, and only in this regime a large increase in S^* is possible when the temperature jump occurs. This suggests that observation of the memory effect requires a large increase of S^* .

The requirements for the observation of the memory effect can be summarized in Fig. 4. Upon isothermal annealing at low temperature, the enthalpy decreases. When the temperature jumps to high temperature, a memory effect will not be observed if the jump occurs into a relaxation region with small S^* . Conversely, the

memory effect will be observed if the jump occurs into a relaxation region with large S^* .

Recent fast scanning calorimetry experiments on the same MG [49] propose an intriguing correlation between the two regimes in Fig. 3(b) with the beta (secondary) relaxation and alpha (primary) relaxation, which allow a physical picture for these results. In the regime of low S^* observed at short annealing times, only the beta relaxation contributes to enthalpy relaxation, while the behavior at longer annealing times (high values of S^*) is associated with the alpha relaxation. The arrow in Fig. 3(c) connects two glasses with the same enthalpy value, but with this enthalpy achieved in two different ways; annealing at low temperature occurs solely via the beta process (optimization of structure via small rearrangements) while annealing at high temperature occurs via the large-scale motion of the alpha process. The memory effect occurs because this glass prepared at low temperature must first abandon its optimized structure, thus initially *increasing* the enthalpy in order to approach equilibrium. On the other hand, jumping into a low S^* state does not result in a memory effect, as the structural optimization that occurred via the beta process during the low temperature step is similar to the optimization that would have occurred during isothermal annealing at high temperature.

It is useful to compare the above understanding of the memory effect to the traditional view based upon heterogeneous dynamics. For metallic and molecular glasses, the two views can be reconciled as a large value of S^* (indicative of a large number of possible escape paths) is indicative of a complex energy landscape for which heterogeneous dynamics can be expected [47,48,50]. For athermal systems, such as crumpled papers and granular materials, we speculate that S^* (or an equivalent quantity that quantifies the connectivity of states in the driven system) will provide important insight into the memory effect. The activation entropy S^* may be proportional to the evolution of states probability $(\partial P/\partial t)(x, t)$, with x being a vector representing the state of an athermal disordered system and t being time, which is consistent with theoretical analysis [34]. The possible role of entropy in memory effects is raised in a review article recently [51]. Our finding suggests that the large activation entropy S^* is essential for the appearance of memory effect.

In summary, the memory effect of an Au-based metallic glass is studied using a high-precision Flash DSC. We find that the memory effect appears only when a temperature jump occurs into a relaxation region with a large S^* . These results are the first experimental evidence for the role of activation entropy in the memory effect of glasses and they provide new understanding of the physical origin of the memory effect. We expect that the activation entropy S^* is a more general and suitable parameter than heterogeneity to characterize the kinetic complexity in various disordered materials regardless of the bonding and packing nature.

Valuable discussions with Dr. Ping Wen are appreciated. We acknowledge financial support from National Key R&D Program of China (2018YFA0703604, 2018YFA0703602), National Natural Science Foundation of China (NSFC 51922102, 51771216, 51701230, 51827801), Zhejiang Provincial Natural Science Foundation of China (LR18E010002), Ningbo 2025 Science and Technology Innovation Project (2019B10051), and the U.S. National Science Foundation through the University of Wisconsin Materials Research Science and Engineering Center (DMR-1720415).

*To who correspondence should be addressed.
jqwang@nimte.ac.cn

- [1] J. Yang, Y. J. Wang, E. Ma, A. Zaccone, L. H. Dai, and M. Q. Jiang, Structural Parameter of Orientational Order to Predict the Boson Vibrational Anomaly in Glasses, *Phys. Rev. Lett.* **122**, 015501 (2019).
- [2] F. Zhu, H. K. Nguyen, S. X. Song, D. P. Aji, A. Hirata, H. Wang, K. Nakajima, and M. W. Chen, Intrinsic correlation between β -relaxation and spatial heterogeneity in a metallic glass, *Nat. Commun.* **7**, 11516 (2016).
- [3] H. B. Yu, W. H. Wang, H. Y. Bai, and K. Samwer, The β -relaxation in metallic glasses, *Nat. Sci. Rev.* **1**, 429 (2014).
- [4] Z. Evenson, S. E. Naleway, S. Wei, O. Gross, J. J. Kruzic, I. Gallino, W. Possart, M. Stommel, and R. Busch, β relaxation and low-temperature aging in a Au-based bulk metallic glass: From elastic properties to atomic-scale structure, *Phys. Rev. B* **89**, 174204 (2014).
- [5] V. M. Boucher, D. Cangialosi, A. Alegria, and J. Colmenero, Complex nonequilibrium dynamics of stacked polystyrene films deep in the glassy state, *J. Chem. Phys.* **146**, 203312 (2017).
- [6] A. J. Kovacs, Transition vitreuse dans les polymères amorphes. Etude phénoménologique, *Adv. Polym. Sci.* **3**, 394 (1963).
- [7] A. Q. Tool, Relaxation between inelastic deformability and thermal expansion of glass in its annealing range, *J. Am. Ceram. Soc.* **29**, 240 (1946).
- [8] O. S. Narayanaswamy, A model of structural relaxation in glass, *J. Am. Ceram. Soc.* **54**, 491 (1971).
- [9] C. T. Moynihan *et al.*, Structural relaxation in vitreous materials, *Ann. N.Y. Acad. Sci.* **279**, 15 (1976).
- [10] A. J. Kovacs, J. J. Aklonis, J. M. Hutchinson, and A. R. Ramos, Isobaric volume and enthalpy recovery of glasses. II. A transparent multiparameter theory, *J. Polym. Sci.* **17**, 1097 (1979).
- [11] L. Grassia, Y. P. Koh, M. Rosa, and S. L. Simon, Complete set of enthalpy recovery data using Flash DSC: experiment and modeling, *Macromolecules* **51**, 1549 (2018).
- [12] A. L. Greer and F. Spaepen, Creep, diffusion, and structural relaxation in metallic glasses, *Ann. N.Y. Acad. Sci.* **371**, 218 (1981).
- [13] M. R. J. Gibbs, J. E. Evetts, and J. A. Leake, Activation energy spectra and relaxation in amorphous materials, *J. Mater. Sci.* **18**, 278 (1983).
- [14] E. Lopez and S. L. Simon, Signatures of structural recovery in polystyrene by nanocalorimetry, *Macromolecules* **49**, 2365 (2016).
- [15] D. P. B. Aji, P. Wen, and G. P. Johari, Memory effect in enthalpy relaxation of two metal-alloy glasses, *J. Non-Cryst. Solids* **353**, 3796 (2007).
- [16] P. Luo, Y. Z. Li, H. Y. Bai, P. Wen, and W. H. Wang, Memory Effect Manifested by a Boson Peak in Metallic Glass, *Phys. Rev. Lett.* **116**, 175901 (2016).
- [17] Y. T. Wang, P. F. Li, and L.-M. Wang, Strong dependence of the hardness on fictive temperatures in far-from-equilibrium $\text{La}_{57.5}\text{Ni}_{12.5}\text{Al}_{17.5}\text{Cu}_{12.5}$ metallic glasses, *Intermetallics* **93**, 197 (2018).
- [18] C. A. Volkert and F. Spaepen, Crossover relaxation of the viscosity of $\text{Pd}_{40}\text{Ni}_{40}\text{P}_{19}\text{Si}_1$ near the glass transition, *Acta Metall.* **37**, 1355 (1989).
- [19] A. Eisenbach, T. Havdala, J. Delahaye, T. Grenet, A. Amir, and A. Frydman, Glassy Dynamics in Disordered Electronic Systems Reveal Striking Thermal Memory Effects, *Phys. Rev. Lett.* **117**, 116601 (2016).
- [20] Y. Lahini, O. Gottesman, A. Amir, and S. M. Rubinstein, Nonmonotonic Aging and Memory Retention in Disordered Mechanical Systems, *Phys. Rev. Lett.* **118**, 085501 (2017).
- [21] L. Boesch, A. Napolitano, and P. B. Macedo, Spectrum of volume relaxation times in B_2O_3 , *J. Am. Ceram. Soc.* **53**, 148 (1970).
- [22] A. Amir, Y. Oreg, and Y. Imry, On relaxations and aging of various glasses, *Proc. Natl. Acad. Sci. U.S.A.* **109**, 1850 (2012).
- [23] E. van Bruggen, E. van der Linden, and M. Habibi, Tailoring relaxation dynamics and mechanical memory of crumpled materials by friction and ductility, *Soft Matter* **15**, 1633 (2019).
- [24] S. Dillavou and S. M. Rubinstein, Nonmonotonic Aging and Memory in a Frictional Interface, *Phys. Rev. Lett.* **120**, 224101 (2018).
- [25] A. Prados and E. Trizac, Kovacs-Like Memory Effect in Driven Granular Gases, *Phys. Rev. Lett.* **112**, 198001 (2014).
- [26] B. Kou, Y. Cao, J. Li, C. Xia, Z. Li, H. Dong, A. Zhang, J. Zhang, W. Kob, and Y. Wang, Granular materials flow like complex fluids, *Nature (London)* **551**, 360 (2017).
- [27] A. Vaknin, Z. Ovadyahu, and M. Pollak, Nonequilibrium field effect and memory in the electron glass, *Phys. Rev. B* **65**, 134208 (2002).
- [28] A. Amir, Y. Oreg, and Y. Imry, Electron glass dynamics, *Annu. Rev. Condens. Matter Phys.* **2**, 235 (2011).
- [29] X. J. Di, K. Z. Win, G. B. McKenna, T. Narita, F. Lequeux, S. R. Pullela, and Z. D. Cheng, Signatures of Structural Recovery in Colloidal Glasses, *Phys. Rev. Lett.* **106**, 095701 (2011).
- [30] S. Banik and G. B. McKenna, Isochoric structural recovery in molecular glasses and its analog in colloidal glasses, *Phys. Rev. E* **97**, 062601 (2018).
- [31] Y. B. Han, A. D. Wang, A. N. He, C. T. Chang, F. S. Li, and X. M. Wang, Improvement of magnetic properties, microstructure and magnetic structure of $\text{Fe}_{73.5}\text{Cu}_1\text{Nb}_3\text{Si}_{15.5}\text{B}_7$ nanocrystalline alloys by two-step annealing process, *J. Mater. Sci. Mater. Electron.* **27**, 3736 (2015).

- [32] R. Richert, Heterogeneous dynamics in liquids: Fluctuations in space and time, *J. Phys. Condens. Matter* **14**, R703 (2002).
- [33] G.B. McKenna and S.L. Simon, 50th anniversary perspective: Challenges in the dynamics and kinetics of glass-forming polymers, *Macromolecules* **50**, 6333 (2017).
- [34] C. A. Plata and A. Prados, Kovacs-like memory effect in athermal systems: Linear response analysis, *Entropy* **19**, 539 (2017).
- [35] S. Pogatscher, P. J. Uggowitzer, and J. F. Löffler, In-situ probing of metallic glass formation and crystallization upon heating and cooling via fast differential scanning calorimetry, *Appl. Phys. Lett.* **104**, 251908 (2014).
- [36] J. Schroers, B. Lohwongwatana, W. L. Johnson, and A. Peker, Gold based bulk metallic glass, *Appl. Phys. Lett.* **87**, 061912 (2005).
- [37] J. M. Pelletier, S. Cardinal, J. C. Qiao, M. Eisenbart, and U. E. Klotz, Main and secondary relaxations in an Au-based bulk metallic glass investigated by mechanical spectroscopy, *J. Alloys Compd.* **684**, 530 (2016).
- [38] J. Q. Wang, Y. Shen, J. H. Perepezko, and M. D. Ediger, Increasing the kinetic stability of bulk metallic glasses, *Acta Mater.* **104**, 25 (2016).
- [39] I. Gallino, D. Cangialosi, Z. Evenson, L. Schmitt, S. Hechler, M. Stolpe, and B. Ruta, Hierarchical aging pathways and reversible fragile-to-strong transition upon annealing of a metallic glass former, *Acta Mater.* **144**, 400 (2018).
- [40] S. van Herwaarden, E. Iervolino, F. van Herwaarden, T. Wijffels, A. Leenaers, and V. Mathot, Design, performance and analysis of thermal lag of the UFS1 twin-calorimeter chip for fast scanning calorimetry using the Mettler-Toledo Flash DSC 1, *Thermochim. Acta* **522**, 46 (2011).
- [41] See Supplemental Material at <http://link.aps.org/supplemental/10.1103/PhysRevLett.125.135501> for the details of experiments and the detailed theoretical model and functions, which includes Refs. [42–47].
- [42] F. W. Cagle and H. Eyring, An application of the absolute reaction rate theory to some problems in annealing, *J. Appl. Phys.* **22**, 771 (1951).
- [43] H. E. Kissinger, Reaction kinetics in differential thermal analysis, *Anal. Chem.* **29**, 1702 (1957).
- [44] U. Geyer, S. Schneider, W. L. Johnson, Y. Qiu, T. A. Tombrello, and M. Macht, Atomic Diffusion in the Supercooled Liquid and Glassy States of the $Zr_{41.2}Ti_{13.8}Cu_{12.5}Ni_{10}Be_{22.5}$ Alloy, *Phys. Rev. Lett.* **75**, 2364 (1995).
- [45] F. Faupel, P. W. Huppe, and K. Ratzke, Pressure Dependence and Isotope Effect of Self-Diffusion in a Metallic Glass, *Phys. Rev. Lett.* **65**, 1219 (1990).
- [46] Y. Fan, T. Iwashita, and T. Egami, How thermally activated deformation starts in metallic glass, *Nat. Commun.* **5**, 5083 (2014).
- [47] H. W. Starkweather, Simple and complex relaxations, *Macromolecules* **14**, 1277 (1981).
- [48] A. Heuer, Exploring the potential energy landscape of glass-forming systems: from inherent structures via metabasins to macroscopic transport, *J. Phys. Condens. Matter* **20**, 373101 (2008).
- [49] L. J. Song, W. Xu, J. T. Huo, J. Q. Wang, X. M. Wang, and R. W. Li, Two-step relaxations in metallic glasses during isothermal annealing, *Intermetallics* **93**, 101 (2018).
- [50] H. W. Starkweather, Distribution of activation enthalpies in viscoelastic relaxations, *Macromolecules* **23**, 328 (1990).
- [51] N. C. Keim, J. D. Paulsen, Z. Zeravcic, S. Sastry, and S. R. Nagel, Memory formation in matter, *Rev. Mod. Phys.* **91**, 035002 (2019).